

**Pneumatic Battery**  
**A Chemical Alternative to Pneumatic Energy**  
**Storage**

by

Nigel Kojimoto

Submitted to the Department of Mechanical Engineering  
in partial fulfillment of the requirements for the degree of

Bachelor of Science in Mechanical Engineering

at the

MASSACHUSETTS INSTITUTE OF TECHNOLOGY

June 2012

© Massachusetts Institute of Technology 2012. All rights reserved.

Author .....  
Department of Mechanical Engineering  
May 22, 2012

Certified by .....  
Daniela Rus  
Professor of Electrical Engineering and Computer Science  
Thesis Supervisor

Accepted by .....  
John H. Lienhard V  
Collins Professor of Mechanical Engineering  
Chairman, Undergraduate Thesis Committee



# Pneumatic Battery

## A Chemical Alternative to Pneumatic Energy Storage

by

Nigel Kojimoto

Submitted to the Department of Mechanical Engineering  
on May 22, 2012, in partial fulfillment of the  
requirements for the degree of  
Bachelor of Science in Mechanical Engineering

### Abstract

Pneumatic power is traditionally provided by compressed air contained in a pressurized vessel. This method of energy storage is analogous to an electrical capacitor. This study sought to create an alternative pneumatic device, the pneumatic battery, that would be analogous to an electrical battery. A pneumatic battery allows energy to be stored chemically in a Hydrogen Peroxide ( $H_2O_2$ ) solution and released when the solution decomposes, producing oxygen gas. This decomposition is sped up with the aid of a platinum catalyst. A mechanical negative feedback system regulates the exposure of the catalyst, allowing the battery to generate a user specified pressure at its outlet. The prototype produced was observed to generate an outlet pressure of up to 470 kPa (68 psi) and is theoretically capable of generating up to 689 kPa (100 psi) with a volumetric energy density greater than that of conventional compressed air tanks.

Thesis Supervisor: Daniela Rus

Title: Professor of Electrical Engineering and Computer Science



## Acknowledgments

The author would like to thank Dr. Cagdas Onal for providing the project's initial inspiration as well for his continued insight and support, Professor Daniela Rus for her sponsorship of the project, and Ron Wiken for his machining expertise. This project would not have been possible without the help of these amazing individuals.



# Contents

<b>1</b>	<b>Introduction</b>	<b>13</b>
1.1	Background . . . . .	14
<b>2</b>	<b>Battery Prototype Design</b>	<b>17</b>
2.1	Battery Components . . . . .	17
2.2	Chemical Analysis . . . . .	23
2.3	Prototype Construction . . . . .	26
<b>3</b>	<b>Battery Prototype Performance</b>	<b>29</b>
3.1	Experimental Methods . . . . .	29
3.2	Results and Discussion . . . . .	30
3.3	Conclusions . . . . .	41
3.3.1	Next Steps . . . . .	41
<b>A</b>	<b>Prototype Part Drawings</b>	<b>43</b>





# List of Figures

2-1	Rendering showing components of the complete pneumatic battery assembly in full and cross sectional views. . . . .	18
2-2	Rendering showing the components of the complete piston assembly. .	18
2-3	Cross-sectional view of the main body, defining the piston bore, catalyst chamber, and solution chamber. . . . .	19
2-4	Battery when catalyst is fully exposed to hydrogen peroxide solution.	20
2-5	Graphic clarifying $x_{knob}$ , the relative distance between the knob and the body, $x_{piston}$ , the relative distance of the piston from the body, and $L$ , the length of the spring. . . . .	21
2-6	Battery when the catalyst gasket contacts the main body, effectively stopping the reaction. . . . .	23
2-7	Plot of estimated volumetric energy densities for a pneumatic battery and SCUBA tank. Note that the volume ratio is irrelevant for the SCUBA tank . . . . .	26
2-8	Picture of the platinum catalysts used after they were turned down. .	28
3-1	Picture showing the set-up of the experiments. . . . .	30
3-2	Plot showing the pneumatic battery's response to a 3% hydrogen peroxide solution and no restoring force from the spring, or a knob position of 0 turns. . . . .	31
3-3	Plot showing the pneumatic battery's response to a 3% hydrogen peroxide solution and a knob position of 1 turn. . . . .	32

3-4	Plot showing the pneumatic battery's response to a 3% hydrogen peroxide solution and a knob position of 2 turns. . . . .	32
3-5	Plot showing the pneumatic battery's response to a 3% hydrogen peroxide solution and a knob position of 3 turns. . . . .	33
3-6	Plot showing the pneumatic battery's response to a 3% hydrogen peroxide solution and a knob position of 4 turns. . . . .	33
3-7	Plot showing the pneumatic battery's response to a 3% hydrogen peroxide solution and a knob position of 5 turns. . . . .	34
3-8	Plot comparing initial battery response to a 3% solution at various knob positions. . . . .	34
3-9	Picture showing the pin extruding from the battery, showing approximately two notch spaces. . . . .	35
3-10	Close up of the pin extruding from the battery, showing approximately four notch spaces. . . . .	36
3-11	Plot showing the pneumatic battery's response to a 10% hydrogen peroxide solution and a knob position of 0 turns. . . . .	37
3-12	Plot showing the pneumatic battery's response to a 10% hydrogen peroxide solution and a knob position of 2 turns. . . . .	37
3-13	Plot showing the pneumatic battery's response to a 10% hydrogen peroxide solution and a knob position of 3 turns. . . . .	38
3-14	Plot of maximum pressure attained at various knob positions and concentrations of hydrogen peroxide. . . . .	39
3-15	Plot showing the pneumatic battery's response to a 50% hydrogen peroxide solution and a knob position of 3 turns. Note that the battery was vented before the pressures were able to stabilize. . . . .	40
3-16	Sketch of an improved battery design. . . . .	42
A-1	Drawing of the cap. . . . .	43
A-2	Drawing of the main body. . . . .	44
A-3	Drawing of the knob. . . . .	45

A-4	Drawing of the piston. . . . .	46
A-5	Drawing of the Clear Care catalyst after turning. . . . .	47
A-6	Drawing of the catalyst mount. . . . .	48
A-7	Drawing of the catalyst cap. . . . .	49
A-8	Drawing of the pin. . . . .	50



# Chapter 1

## Introduction

Pneumatic power is traditionally provided by utilizing compressed air contained in a pressurized vessel to perform mechanical work. This method of energy storage is similar to that of an electrical capacitor. The more gas that is desired, the greater the pressure inside the vessel, the harder it becomes to store more gas. Additionally, in the case of pneumatics, the structural strength and fatigue life of the containing vessel limits the containable pressure. These factors limit the amount and duration of pressure that a conventional vessel can provide.

This study sought to create an alternative pneumatic device, the pneumatic battery, that would be a pneumatic equivalent to an electrical battery. A pneumatic battery utilizes a chemical solution to produce the desired gas through a chemical reaction, sped up with the aid of a catalyst. By regulating the exposure of a catalyst, the pneumatic battery is able to generate a desired pressure at its outlet. By storing the gas chemically, it is possible for more gas to be released than in air tanks of comparable size, while at the same time experiencing smaller internal pressures.

The battery produced for this study utilizes a hydrogen peroxide ( $H_2O_2$ ) chemical decomposition sped up by a platinum catalyst to create oxygen gas. Such a device could have numerous applications in various fields. Listed below are a few ways a refined pneumatic battery could be useful.

Hydrogen peroxide decomposition has already been implemented in rocketry. If the battery was large enough, it could maintain its outlet pressure while keeping

the decomposition rate constant by varying catalyst exposure, despite a decreasing concentration of hydrogen peroxide.

With a higher volumetric energy density, a pneumatic battery could replace conventional air cylinders and canisters. This could make portable pneumatic tools more viable. They could be used to do anything from topping off tires to spraying dust out of a keyboard to tetherless power tools. Because the battery could be set to generate zero pressure, the working hydrogen peroxide can be easily replaced, eliminating the need for larger refill tanks, cartridge refills or pumps. Plus, they could be stored with zero internal gauge pressure, making them much safer.

The increased volumetric energy density factor could make the pneumatic battery very attractive for powering mobile pneumatic robots. Robots could be designed to be much more compact without larger air tanks.

In the field of scuba diving, pneumatic batteries could serve as a replacement for oxygen tanks. Since the battery could be at a lower gauge pressure, it could serve as a thinner walled replacement while providing more oxygen overall.

These are just a few of the many applications this new technology could have. The pneumatic battery has the potential to change the way we view pneumatics. This study outlines the creation and testing of a pneumatic battery prototype. Section 1.1 provides information on the uses of hydrogen peroxide decomposition and previously designed alternative pneumatic power sources. Section 2 details the design and construction of the pneumatic battery prototype. Section 3.1 details the design of experiments used to test the prototype performance. The results of performance tests are presented in Section 3.2 and finally a conclusion is given in Section 3.3.

## 1.1 Background

The decomposition of hydrogen peroxide is a well studied chemical reaction that speeds up in the presences of a catalyst, details of which can be found in [5]. The fast nature of this decomposition at high concentrations has led to hydrogen peroxide's use as a monopropellant for rocket applications [8]. More recently it has been used in

various robotic applications [6], [7], and has even been used to power a microfluidic chip [4].

Pneumatic actuation is not new for robotic applications, and a brief overview can be found in [2]. The concept of using hydrogen peroxide decomposition to power robots has been previously explored in [1], where desired pressures were achieved by controlling the contact between a catalyst and flowing hydrogen peroxide solution with a binary solenoid valve. Their proposed system claimed to have the potential for an order of magnitude improvement in actuation potential over a battery powered DC motor approach

The concept of an integrated pneumatic battery is very new. The first development of such a device utilized a soft membrane seal and was built for pneumatic robotic systems [3]. This initial prototype was built from acrylic and was capable of generating up to 206.8 kPa (30 psi) of pressure, and observed to generate 68.9 kPa (10 psi). This study sought to improve upon the performance of that battery.





# Chapter 2

## Battery Prototype Design

This chapter will detail the design and fabrication of the pneumatic battery constructed for this study. Section 2.1 is an in depth discussion of the design and mechanics of individual components. Section 2.2 details the chemical process and design of the battery, as well as volumetric energy density estimates. Section 2.3 details the fabrication decisions of the battery prototype.

### 2.1 Battery Components

The various components of the pneumatic battery can be found in Fig. 2-1 and 2-2. The battery consists of 15 parts, each of which serves a specific purpose. The main body serves as the structure of the battery and contains the piston bore, catalyst chamber, and hydrogen peroxide solution chamber, as defined in Fig. 2-3. The cap contains the solution chamber and provides the battery outlet, a fitting to which tubing can be attached. The cap gaskets provide the seal between the body and the cap, containing any internal pressure and solution. The filter prevents hydrogen peroxide solution from exiting the battery outlet, while allowing gas to pass through. The knob allows the zero position of the spring to change and the pin acts as a mechanical readout of the pressure inside the battery.

The components of the piston assembly are as follows. The piston mounts the catalyst, allowing it to move between the catalyst chamber and the solution chamber.

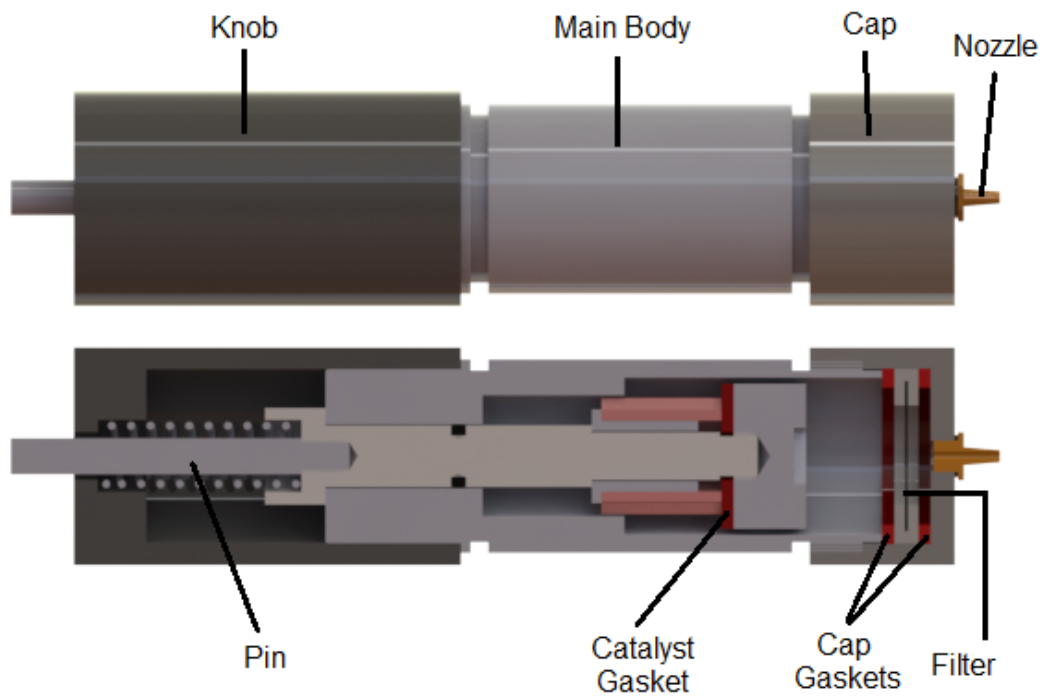


Figure 2-1: Rendering showing components of the complete pneumatic battery assembly in full and cross sectional views.

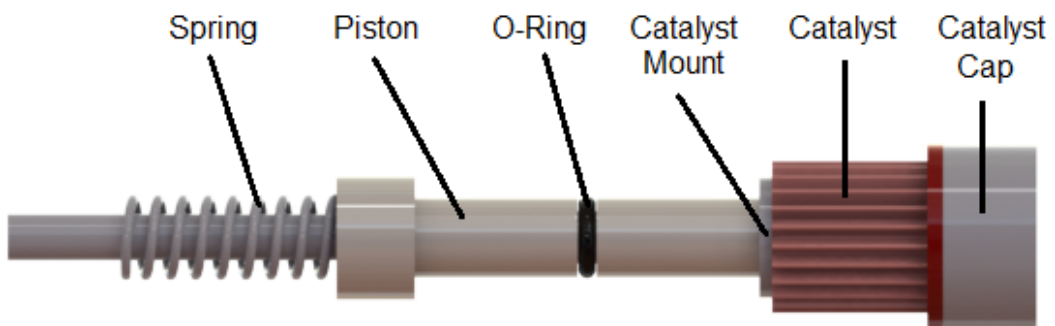


Figure 2-2: Rendering showing the components of the complete piston assembly.

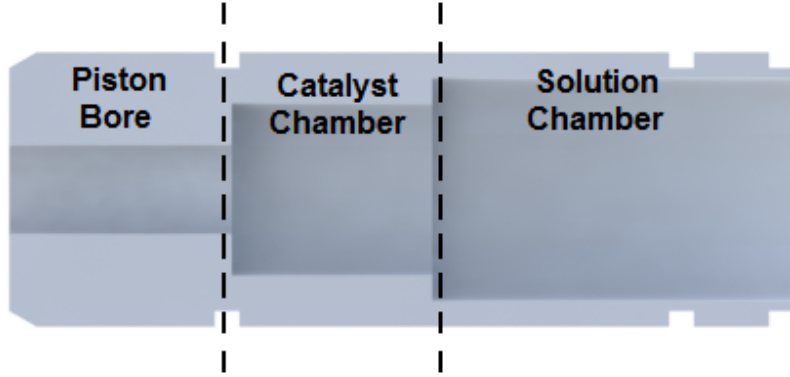


Figure 2-3: Cross-sectional view of the main body, defining the piston bore, catalyst chamber, and solution chamber.

The piston O-ring provides a seal between the piston and the piston bore, preventing the hydrogen peroxide solution from leaking out. The catalyst significantly increases the rate at which hydrogen peroxide decomposes into water and oxygen gas. The catalyst mount allows the catalyst to be mounted onto the piston. The combination of the catalyst cap and catalyst gasket, also mounted on the piston, provides a dynamic barrier between the catalyst chamber and solution chamber. The spring provides a restoring force on the piston when in compression.

The working mechanism behind the battery goes as follows. The piston is oriented such that the catalyst rests inside the solution chamber, as shown in Fig. 2-4. As the catalyst interacts with a hydrogen peroxide solution, oxygen gas is produced, causing the internal battery pressure to rise. For the piston to be in static equilibrium,

$$PA_b + F_{friction} + F_{spring} + F_{body} = 0, \quad (2.1)$$

must hold true, where  $P$  is the gauge pressure of the battery,  $A_b$  is the cross sectional area of the piston bore,  $F_{friction}$  is the frictional force on the piston,  $F_{spring}$  is the restoring force on the piston by the spring, and  $F_{body}$  is the contact force between the catalyst gasket and the main body. Note that the only time  $F_{body}$  can be non-zero is when there is contact between the catalyst gasket and the main body.

Because one side of the piston is exposed to the internal battery pressure while

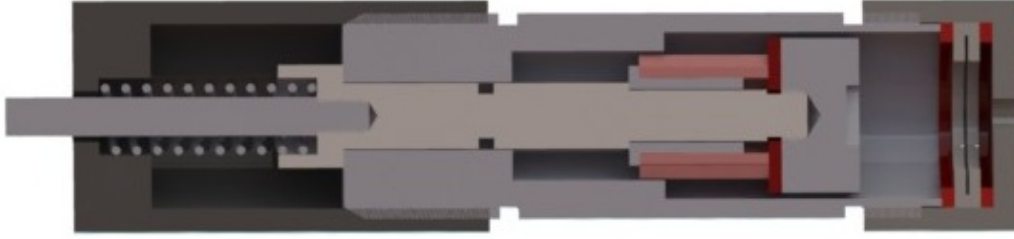


Figure 2-4: Battery when catalyst is fully exposed to hydrogen peroxide solution.

the other is exposed to the atmosphere, the resulting pressure difference across the piston causes it to move, pulling the catalyst into the catalyst chamber. Eq. (2.1) can be rewritten to give the condition for piston movement, where

$$|PA_b - (F_{spring} + F_{body})| > F_{friction}. \quad (2.2)$$

Because both  $F_{spring}$  and  $F_{body}$  are contact forces, they will always be oriented in the same direction. The piston continues to move until the catalyst cap and gasket contact the main body, separating the catalyst and solution chambers. The pressure at which the piston stops can be found by rearranging Eq. (2.1), such that

$$P = \frac{F_{friction} + F_{spring} + F_{body}}{A_b}. \quad (2.3)$$

The restoring force provided by the spring can be expressed using Hooke's law as

$$F_{spring} = \max(0, k\Delta x), \quad (2.4)$$

where  $k$  is the spring constant of the compression spring, and  $\Delta x$  is the amount by which the spring has been compressed. Through inspection,  $\Delta x$  can be written as

$$\Delta x = (L - x_{knob} + x_{piston}), \quad (2.5)$$

where  $x_{knob}$  is the relative distance between the knob and the body,  $x_{piston}$  is the relative distance of the piston from the body, and  $L$  is the length of the spring, as

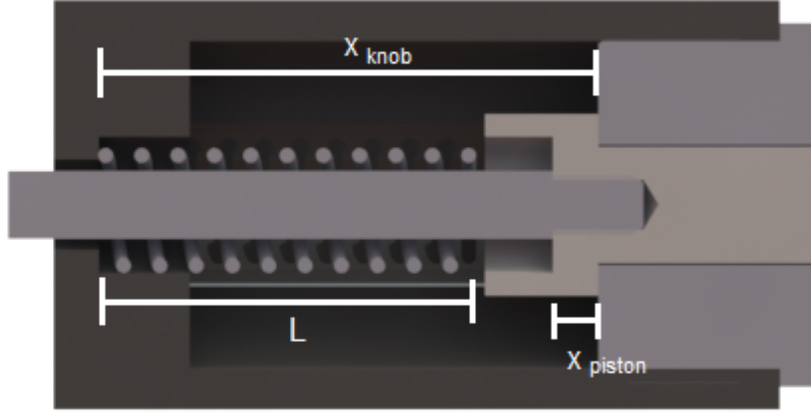


Figure 2-5: Graphic clarifying  $x_{knob}$ , the relative distance between the knob and the body,  $x_{piston}$ , the relative distance of the piston from the body, and  $L$ , the length of the spring.

shown in Fig. 2-5. Substituting Eq. (2.5) into (2.4), we get

$$F_{spring} = \max(0, k(L - x_{knob} + x_{piston})). \quad (2.6)$$

Eq. (2.6) shows that if  $L - x_{knob} + x_{piston} < 0$ , then  $F_{spring}$  will be zero. Thus, we can guarantee that the spring does not provide a restoring force by setting the knob such that  $x_{knob} > L + x_{p,max}$ , where  $x_{p,max}$  is the maximum possible value of  $x_{piston}$ .

When the catalyst gasket first comes into contact with the main body,  $F_{body}$  can be approximated as being 0. Under a condition of zero spring and body forces, we revisit Eq. (2.3), to get

$$P_{min} = \frac{F_{friction}}{A_b}. \quad (2.7)$$

Eq. (2.7) gives  $P_{min}$ , the lowest pressure the battery can output. By substituting Eq. (2.6) into (2.3) and rearranging, we can find the outlet pressure  $P$  at equilibrium for a given knob position  $x_{knob}$  to be,

$$P = \frac{F_{friction} + F_{body} + k(L - x_{knob} + x_{p,max})}{A_b}, \quad (2.8)$$

assuming that the value of  $x_{knob}$  is such that it causes compression of the spring. The maximum outlet pressure of the battery,  $P_{max}$ , occurs when the deflection of the spring,  $\Delta x$ , is at its maximum of  $\Delta x_{max}$ . This occurs when the knob is set, such that,

$$x_{knob} = L + x_{p,max} - \Delta x_{max} \quad (2.9)$$

and yields an outlet pressure of

$$P_{max} = \frac{F_{friction} + F_{body} + k\Delta x_{max}}{A_b}. \quad (2.10)$$

After the catalyst cap and gasket make initial contact with the body, as shown in Fig. 2-6, any hydrogen peroxide solution remaining inside the catalyst chamber is displaced by additional bubbles, increasing the pressure inside the catalyst chamber relative to the solution chamber. This creates a pressure difference between the catalyst chamber and solution chamber, causing the seal between the catalyst gasket and main body to break, intermittently venting excess solution and gas into the solution chamber and re-establishing the seal once that pressure difference is nullified. The seal is re-established because there still exists the original pressure difference over the piston. For the remainder of this paper, this process will be referred to as the venting effect. This venting effect continues until there is no longer any reacting solution in the catalyst chamber, and it is this venting process that gives  $F_{body}$  a non zero value.  $F_{body}$  is unfortunately difficult to predict, and if a better method of stopping the reaction was developed, the magnitude of  $F_{body}$  could become negligibly small.

Note the difference between pin positions relative to the knob in Fig. 2-4 and 2-6, and how the pin is sticking out much more in Fig. 2-6. This is because the distance that the pin sticks out of the knob is a constant value offset from the compression of the spring. Because the amount of spring compression relates to the internal pressure of the battery, the amount the pin sticks out can actually be used as a coarse measurement of the internal pressure of the battery.

Once the presence of reacting solution in the catalyst chamber is gone, the device

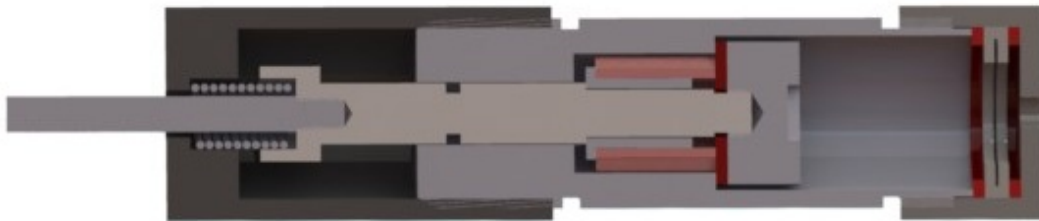


Figure 2-6: Battery when the catalyst gasket contacts the main body, effectively stopping the reaction.

maintains its internal pressure until the built up compressed gas is used. At this point, the internal pressure of the battery drops to atmospheric, nullifying the previously held pressure difference. The spring then provides a restoring force, re-exposing the catalyst to the solution.

This pneumatic battery design introduces a few improvements on previous designs. First of all, this battery was machined from aluminum, increasing its capacity to safely hold higher pressures. This new battery was designed to safely operate at a gauge pressure of up to 689 kPa (100 psi). Second, a new adjustable mechanical feedback system was utilized. The use of the knob allows the user to change the zero position of the spring, effectively choosing the cut-off pressure for the chemical reaction. This allows the cut-off pressure to be easily varied between 0-689 kPa (0-100psi). Last, the use of the pin as a mechanical readout allows the user to have a course idea of how the battery is performing.

## 2.2 Chemical Analysis

The decomposing hydrogen peroxide obeys the following the equation,



Although this reaction occurs naturally, it is greatly sped up with the aid of a catalyst. Platinum was chosen as the catalyst for a number of reasons. In previous studies, [3], although silver served as a good catalyst, it had problems oxidizing when exposed

to air, poisoning its catalytic capabilities. Platinum was suggested as a solution as it is not subject to the same oxidization problem. The use of a catalyst for this decomposition in general is very beneficial. It greatly speeds up the reaction and is reusable over and over. The reuseability of a catalyst is only limited by the wear on the catalyst, and can thus in theory last for a significantly long time.

The total energy storable in the battery can be estimated with the following method. If  $c$  is the percent concentration of hydrogen peroxide ( $g/100ml$ ),  $V_f$  is the initial loaded volume of hydrogen peroxide fluid solution, and  $M$  is the molar mass of hydrogen peroxide, the initial moles of hydrogen peroxide in the solution,  $m_{H_2O_2}$ , can be written as

$$m_{H_2O_2} = \frac{cV_f}{M}. \quad (2.12)$$

If  $e$  is the percentage of hydrogen peroxide that decomposes, the moles of oxygen gas produced,  $m_{O_2}$ , can be written as

$$m_{O_2} = \frac{ecV_f}{2M}, \quad (2.13)$$

with the factor of 2 coming from Eq. (2.11).

Once the battery has reached an equilibrium pressure, and has had time to reach thermal equilibrium with its environment, we can calculate the maximum energy stored that could be released in an isothermal process,

$$E = PV_g \ln \frac{P}{P_0}, \quad (2.14)$$

where  $E$  is the stored energy,  $P$  is the pressure of the produced gas,  $P_0$  is the ambient pressure, and  $V_g$  is the gas volume inside the battery. Using the ideal gas law,

$$PV_g = m_{O_2}RT, \quad (2.15)$$

where  $R$  is the ideal gas constant, and  $T$  is the temperature of the gas, we can



substitute into Eq. (2.14) to obtain

$$E = m_{O_2} RT \ln \frac{m_{O_2} RT}{P_0 V_g}. \quad (2.16)$$

We can then substitute Eq. (2.13) into (2.16), and divide by the total internal volume of the battery  $V$ , to obtain,

$$\epsilon = \frac{ecV_f}{2MV} RT \ln \left( \frac{ecV_f RT}{2MP_0 V_g} \right), \quad (2.17)$$

where  $\epsilon$  is the volumetric energy density of pneumatic battery solution and gas, and  $V = V_g + V_f$ . If we introduce a new dimensionless parameter  $v$ , the volume ratio, such that,

$$v = \frac{V_f}{V}, \quad (2.18)$$

we can rewrite Eq. (2.17) in the form,

$$\epsilon = \frac{ecv}{2M} RT \ln \left( \frac{ecRT}{2MP_0} \frac{v}{1-v} \right). \quad (2.19)$$

We can use Eq. (2.19) to estimate the total volumetric energy stored in a pneumatic battery, or the energy that the battery would have if all of the hydrogen peroxide decomposed into water and oxygen gas per unit of internal volume. Using  $R = 8.31 J/Kmol$ ,  $e = 1.0$ ,  $M = 34g/mol$ ,  $P_0 = 10^5 Pa$ ,  $T = 293^\circ K$ , and varying  $c$  and  $v$ , we obtain the estimated volumetric energy density curves found in Fig. 2-7.

This can be compared to the volumetric energy density of a SCUBA tank, which is commonly rated up to about 20 MPa (3000 psi). By using Eq. (2.14) and dividing by  $V_g$ , we can estimate the volumetric energy density of a SCUBA tank to be:

$$\epsilon = (20MPa) \ln \left( \frac{20MPa}{0.1MPa} \right) = 110MJ/m^3. \quad (2.20)$$

This value is compared to the pneumatic battery's volumetric energy density curves in Fig. 2-7.

Looking at Fig. 2-7, it is clear that the pneumatic battery is capable of storing

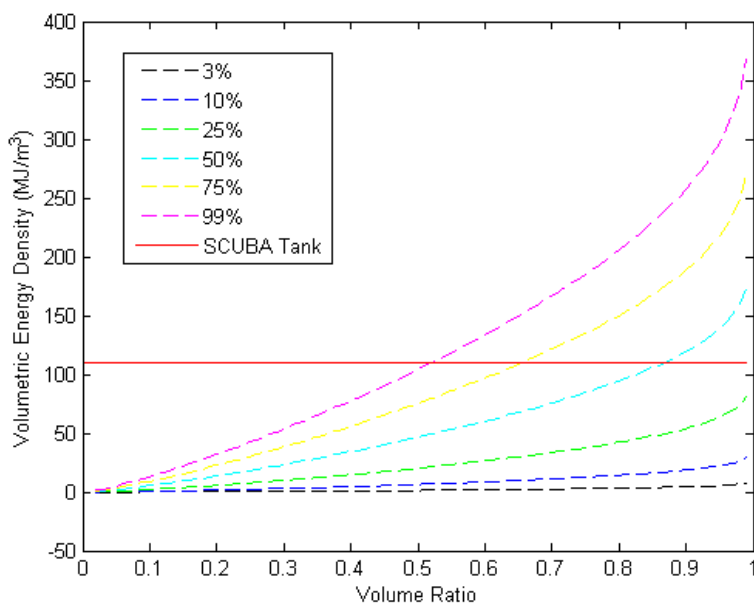


Figure 2-7: Plot of estimated volumetric energy densities for a pneumatic battery and SCUBA tank. Note that the volume ratio is irrelevant for the SCUBA tank

volumetric energy densities larger than that of a SCUBA tank for larger concentrations of hydrogen peroxide. Additionally, because this analysis assumed thermal equilibrium of stored gas with the environment, it is actually an underestimate of the total potential energy. This is because the decomposition reaction of hydrogen peroxide is an exothermic process, meaning that gas is produced at a greater temperature than the environment, adding another element to the releasable energy if the built up pressure is used quickly.

## 2.3 Prototype Construction

The completed battery prototype can be seen in Fig. 3-1. Almost all of the parts for this iteration of the pneumatic battery were machined from 6061T6 Aluminum stock. These parts included the main body, cap, piston, catalyst cap, catalyst mount, knob, and pin. Part drawings for these components can be found in appendix A. Aluminum was chosen for its known stability with large concentrations of hydrogen peroxide, as

well as for being lightweight, relatively inexpensive, and easy to machine. The knob and main body were given 1"-12 threads, allowing the knob a linear movement of approximately 2.1mm/turn (0.0833 in). The back of the knob was rounded out to remove unnecessary material, making it lighter. Knurals were added to the body, cap, and knob to make the parts easier to grip and tighten by hand. A notch in the catalyst cap allows it to be easily screwed onto the piston.

Knurals were also added to the back of the pin to make it easy to grasp, as shown in Fig. 3-10. Notches were also added to pin, to serve as a mechanical readout of the pressure. The notches on the pin are placed 1.27mm (0.05in) apart and were intended to correspond to increments of 68.9 kPa (10psi), with the bottommost notch indicating the "zero" internal pressure state. Thus, this gauge works similar to a ruler, such that the distance between the bottommost notch and the knob indicates the internal pressure.

The cap gaskets were made by laser cutting 1/16" EPDM rubber, while the catalyst gasket was made by molding silicone rubber. The nozzle fitting, o-ring, and compression spring were all purchased as finished parts. The chosen nozzle was a brass fitting that included its own gasket. The chosen spring was made of stainless steel and had an uncompressed length of 2.54 cm (1 in), and a stiffness of 28.6 N/cm (16.3 lbs/in). A Viton Fluorelastomer O-ring was chosen for its stability with high concentrations of hydrogen peroxide. The catalyst was adapted from Clear Care, a contact lens cleaning product. The kit contains a plastic piece that is coated with a thin layer of platinum catalyst. The outer diameter of the catalysts were turned down to make them more compact, as shown in Fig. 2-8.



Figure 2-8: Picture of the platinum catalysts used after they were turned down.

# Chapter 3

## Battery Prototype Performance

### 3.1 Experimental Methods

To test the Pneumatic battery an acrylic stand was constructed, as shown in Fig. 3-1. Tubing connects the battery nozzle to a Honeywell ASDX100D44R pressure sensor. The sensor is capable of measuring between 0-689kPa (0-100psi). The sensor was connected to an NI USB-6008 data acquisition device. The battery was loaded with 5 ml of hydrogen peroxide solution at concentrations including 3%, 10% and 50%. The solution was added with a syringe to both measure the input volume and to control the solution filling point to be the boundary between the catalyst chamber and solution chamber, beside the catalysts. This helps to prevent large bubbles from forming between the catalyst and catalyst gasket, which can happen when the solution is simply poured in over the catalyst cap. Large bubbles are undesirable because they decrease the working surface area of the catalyst that is in contact with the solution.

Gauge pressure at the battery outlet was recorded for 6 different knob positions, in increments of single complete rotations of the knob, with 6 turns away from maximum knob position referred to as 0 turns. This is also the position in which the uncompressed spring just begins to contact both the knob and the piston. This way, the number of turns correlates with the pressure output, with 0 turns corresponding to the minimum pressure output and 6 turns corresponding to the maximum pressure output. Each turn corresponds to approximately 2.1mm (0.083in) increment varia-

tions in  $x_{knob}$ . Gauge pressure data was constantly taken as the outlet pressure of the battery stabilized, at which point the battery was vented. The pin was then pushed back into the battery, repositioning the catalyst in the center of the solution chamber, and the process repeated. To check for leaks, the battery was also submerged in water once it had reached an equilibrium pressure. This ensured that any recorded equilibrium was the result of the negative feedback pressure regulation system and not the result of the gas generation rate reaching equilibrium with a gas leak rate.



Figure 3-1: Picture showing the set-up of the experiments.

## 3.2 Results and Discussion

Fig. 3-2–3-7 show experimental results utilizing a 3% hydrogen peroxide solution at various knob positions, while Fig. 3-8 compares the initial response of the battery at different knob positions. They demonstrate that the battery is able to attain different outlet pressures through knob variation. They also show that the rate of pressure

generation does slow down, asymptotically approaching steady state. Unfortunately, the time-scales shown are relatively large, suggesting that a 3% solution may not be able to release its potential energy fast enough for certain applications. However, this pressure generation rate could also be increased by using a catalyst with a larger surface area or by adding a mixing mechanism to prevent the occurrence of large concentration gradients within the hydrogen peroxide. Also, especially apparent in graphs recorded for larger knob positions, after the initial convergence to a single pressure occurs, subsequent convergences occur at significantly lower pressures. This could be the result of not having enough hydrogen peroxide solution or due to a concentration gradient that appears within the solution, with lower concentrations being created closer to the catalyst. Never the less, these tests prove that fairly significant pressures can be generated even when using a readily available 3% hydrogen peroxide solution.

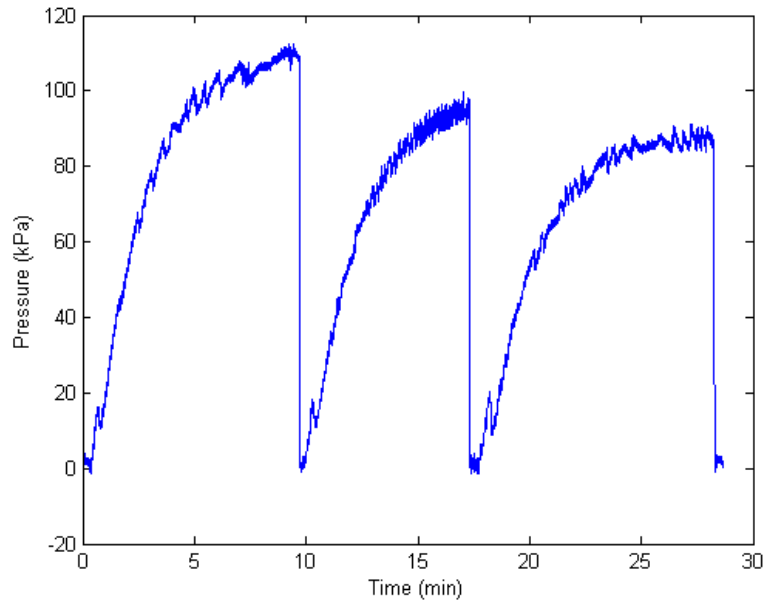


Figure 3-2: Plot showing the pneumatic battery's response to a 3% hydrogen peroxide solution and no restoring force from the spring, or a knob position of 0 turns.

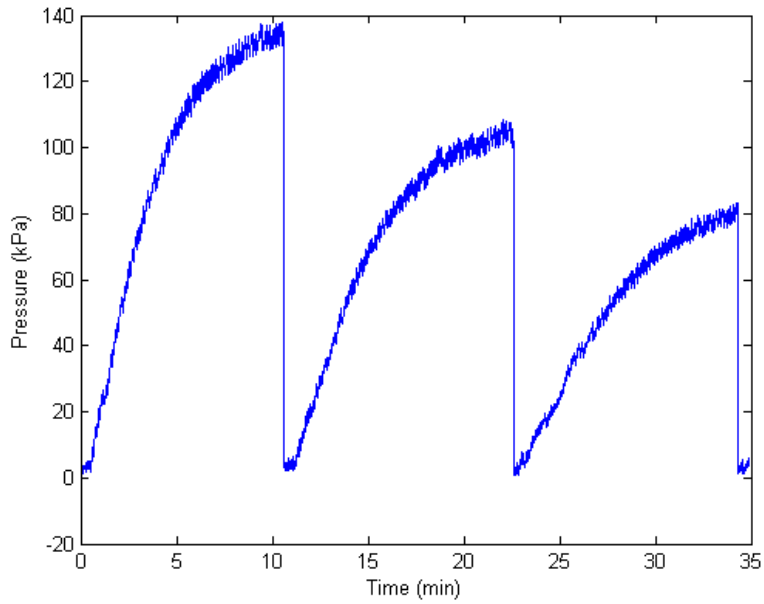


Figure 3-3: Plot showing the pneumatic battery's response to a 3% hydrogen peroxide solution and a knob position of 1 turn.

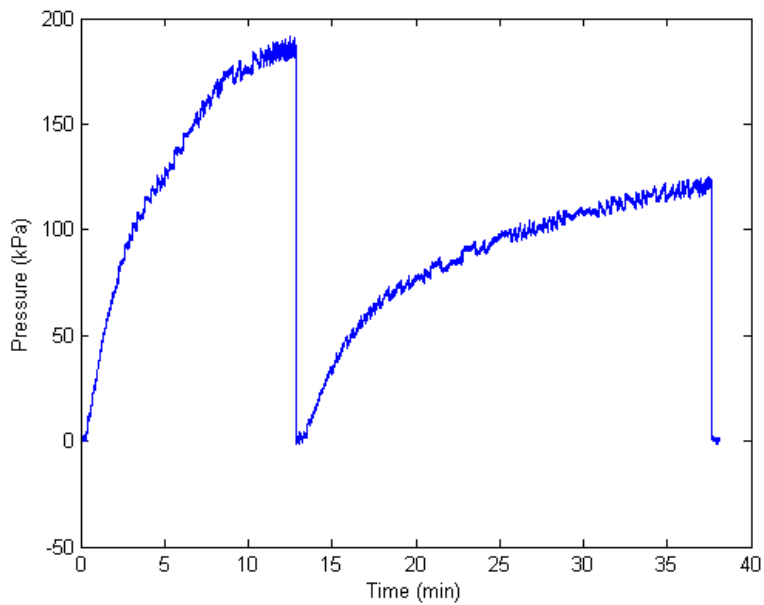


Figure 3-4: Plot showing the pneumatic battery's response to a 3% hydrogen peroxide solution and a knob position of 2 turns.



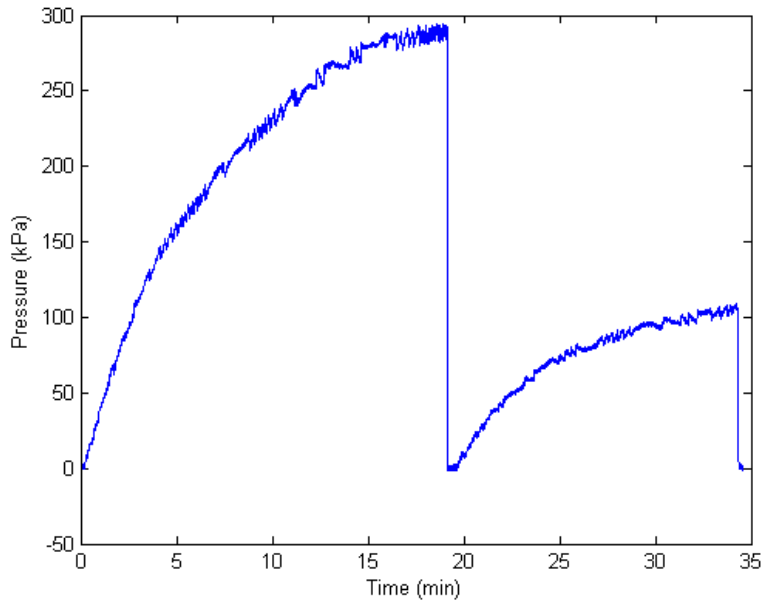


Figure 3-5: Plot showing the pneumatic battery's response to a 3% hydrogen peroxide solution and a knob position of 3 turns.

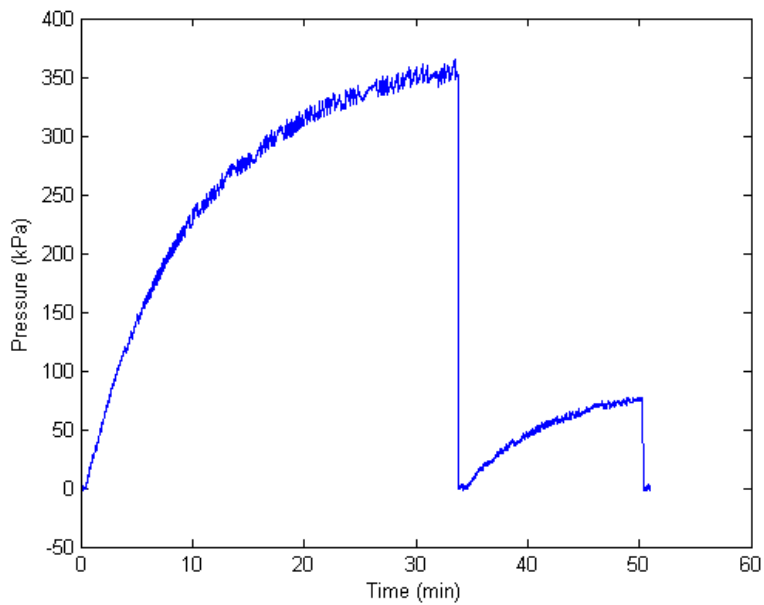


Figure 3-6: Plot showing the pneumatic battery's response to a 3% hydrogen peroxide solution and a knob position of 4 turns.

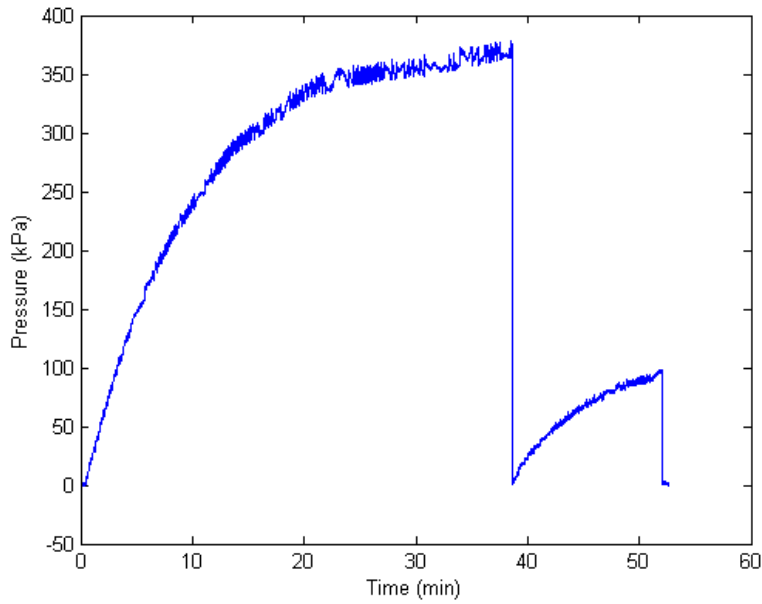


Figure 3-7: Plot showing the pneumatic battery's response to a 3% hydrogen peroxide solution and a knob position of 5 turns.

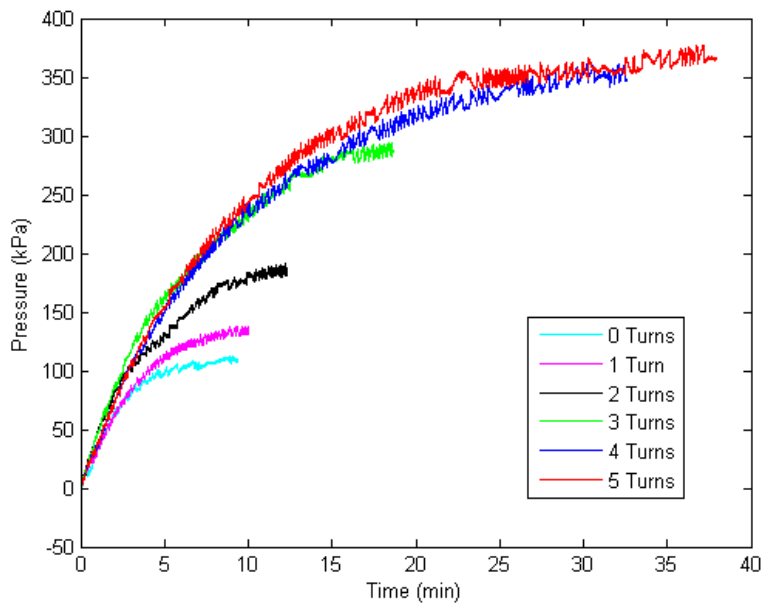


Figure 3-8: Plot comparing initial battery response to a 3% solution at various knob positions.

Fig. 3-9 and 3-10 show the pin at different positions relative to the knob, corresponding to different internal pressures in the battery, showing that the piston was indeed moving. Fig. 3-10 was actually taken when the battery was pressurized to approximately 275 kPa (40 psi), as measured by the pressure sensor. Because roughly four notch spaces are visible in Fig. 3-10, this corresponds to a pressure of about 275 kPa (40 psi), which is what was measured by the sensor. Thus, the pin gauge mechanism was performing correctly in this instance. Unfortunately, the implemented pin gauge design fails when a significant amount of pressure is built up from the venting effect. This is because the pin reaches a maximum extension when the catalyst gasket contacts the main body. It is thus not able to measure additional pressure that is built up after this point. It is also not accurate before the piston starts to move, because friction prevents the piston and therefore the pin from moving while pressure builds up inside the chamber. Nevertheless, it was a useful yet simple mechanism to implement as it gave rough insight as to what was occurring inside the battery.



Figure 3-9: Picture showing the pin extruding from the battery, showing approximately two notch spaces.

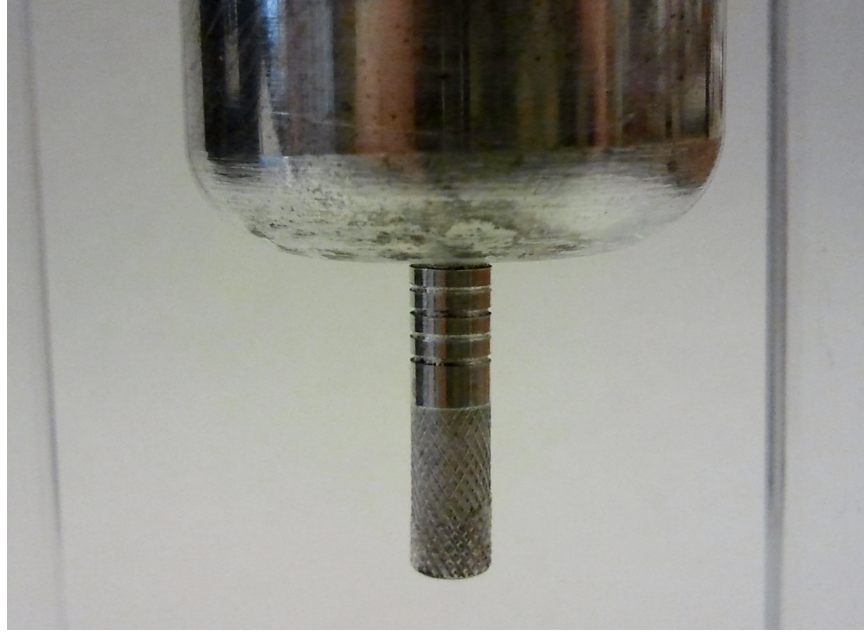


Figure 3-10: Close up of the pin extruding from the battery, showing approximately four notch spaces.

Fig. 3-11–3-13 show the battery’s response when loaded with a 10% hydrogen peroxide solution, at various knob positions. Compared to responses with the 3% solution, the reaction occurs much faster. However, it also reaches significantly higher equilibrium pressures for the same knob position. This suggests that the venting effect of the catalyst cap is actually having a significant effect on the output pressure.

Note that in Fig. 3-13, the second instance of pressure build up is much smaller than the third and fourth. This occurred because the pin was not pushed completely back into the battery. Instead, the spring was relied upon to reposition the catalyst into the solution chamber. Although the spring did cause the piston to move back a small amount, it did not cause the entire motion possible when manually pushing the pin. The fact that the re-exposure to the hydrogen peroxide through the spring does not generate the same response as the when the pin is manually pushed suggests that pushing the pin manually either causes the solution to mix more, or exposes the higher concentrations of hydrogen peroxide in a concentration gradient that exist because of previous pressure building processes.

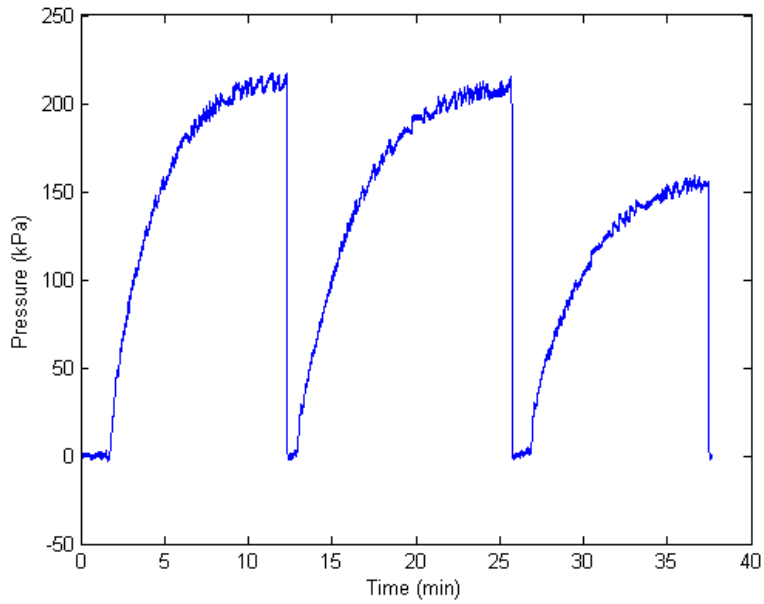


Figure 3-11: Plot showing the pneumatic battery's response to a 10% hydrogen peroxide solution and a knob position of 0 turns.

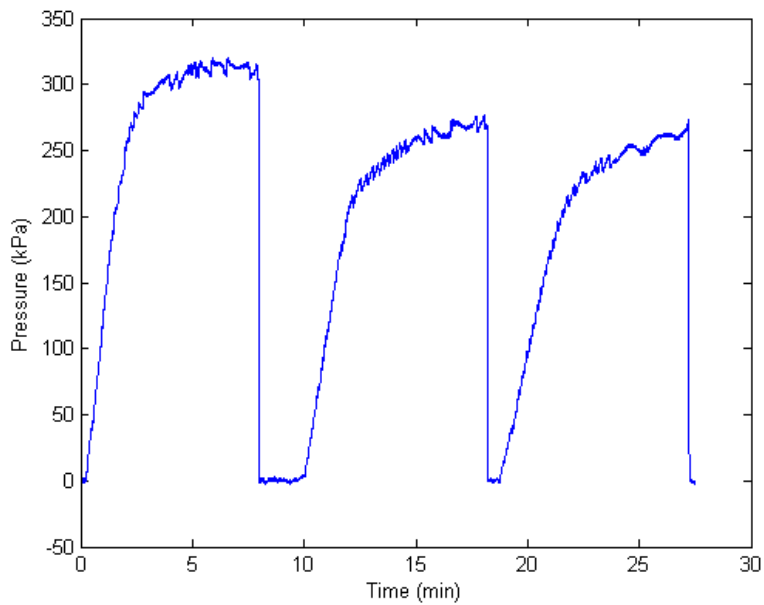


Figure 3-12: Plot showing the pneumatic battery's response to a 10% hydrogen peroxide solution and a knob position of 2 turns.

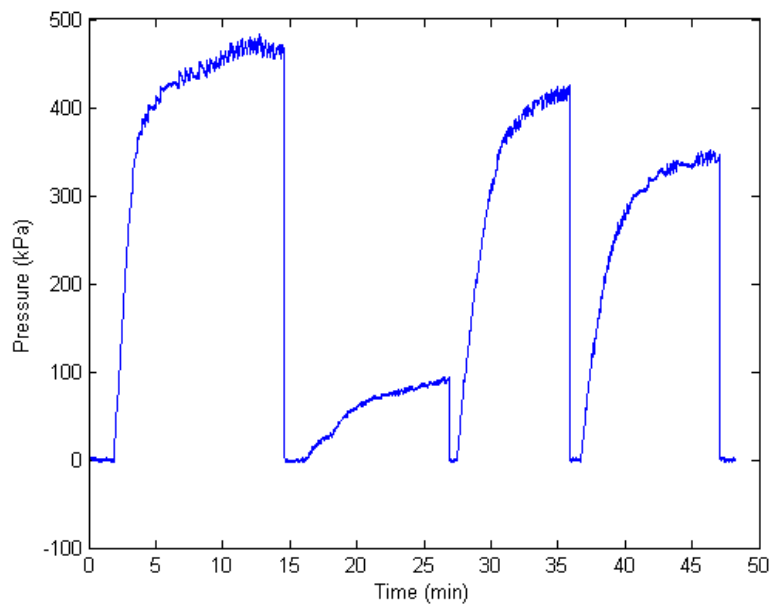


Figure 3-13: Plot showing the pneumatic battery's response to a 10% hydrogen peroxide solution and a knob position of 3 turns.

Fig. 3-14 shows the maximum pressure measured at various knob positions for different concentrations of hydrogen peroxide. It also includes the result of the model given by Eq. (2.10) presented in Section 2.1, but does not take into account the body force,  $F_{body}$ , created by the venting effect. The static friction between the body and the O-ring,  $F_{friction}$ , was measured to be 0.86 N, and this value is included in the model.

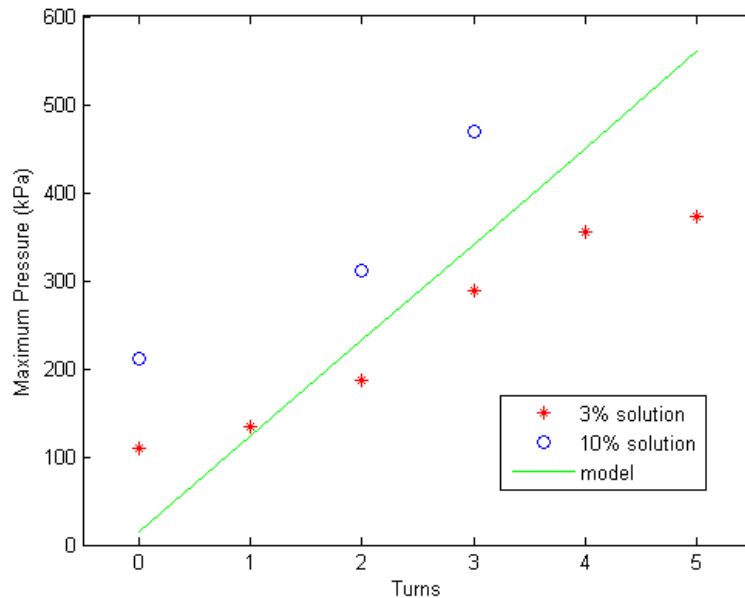


Figure 3-14: Plot of maximum pressure attained at various knob positions and concentrations of hydrogen peroxide.

Fig. 3-14 shows that the venting effect is having a significant effect on the equilibrium pressure, and suggests that gas generated in the catalyst chamber is not displacing the trapped solution. This is suggested by the fact that there is an increase in equilibrium pressure for an increase in solution concentration, when the only change should be in the rate of the reaction. This means that the reaction approaches equilibrium only when the hydrogen peroxide inside the catalyst chamber is completely decomposed. However, because we do reach an equilibrium, we can infer that although the catalyst gasket does allow air generated in the catalyst chamber to escape, it does not allow additional solution from the solution chamber to seep in.

This overshoot from the venting effect could be lessened by having the catalyst chamber conform to the shape of the catalyst more, decreasing the volume of hydrogen peroxide solution that could be trapped.

Another notable aspect of Fig. 3-14 is that for a larger number of turns, the measured maximum pressure of the 3% solution is smaller than the model prediction. Mechanically, there is no good explanation for this. Instead, coupled with the fact that subsequent convergences occur at significantly lower pressures than initial convergences for the 3% solution at a higher number of turns, the measured pressures were likely lower due to a decrease in the concentration of hydrogen peroxide. There may also be some sort of chemical mechanism that decreases the reaction rate of low concentrations of hydrogen peroxide at higher pressures.

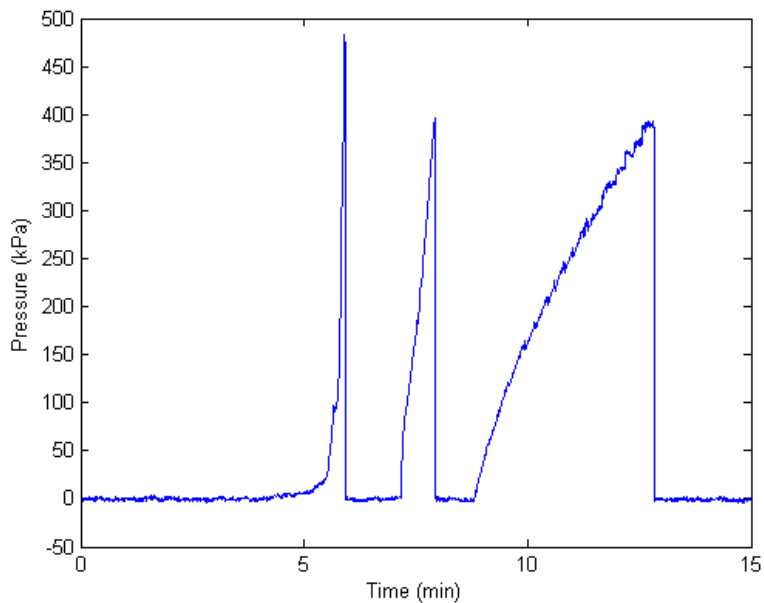


Figure 3-15: Plot showing the pneumatic battery's response to a 50% hydrogen peroxide solution and a knob position of 3 turns. Note that the battery was vented before the pressures were able to stabilize.

Fig. 3-15 shows the response of the battery when loaded with a 50% solution and a knob position of 0 turns. This was the only knob position that was tested, because the battery did not show an indication of reaching an equilibrium pressure below the 689 kPa (100 psi) that the battery was designed to hold. However, Fig. 3-15 does



show a large decrease in the time it takes to build up a significant amount of pressure. Thus, if an improved stopping mechanism for the reaction can be implemented, higher concentrations of hydrogen peroxide could be very useful for applications that require faster pressure recharge rates, or even constant pressure output.

### 3.3 Conclusions

A working pneumatic battery prototype was designed and created for this study that, although not yet ideal, improved upon previous designs. The battery utilized the decomposition of hydrogen peroxide solution ( $H_2O_2$ ) into water and oxygen gas to generate pressure. The decomposition was sped up by a catalyst, whose exposure was controlled by a mechanical negative feedback system. The battery was theoretically capable of generating up to 689 kPa (100 psi) and was observed to generate 479 kPa (68 psi). However, although the battery was able to regulate the reaction, there was significant overshoot of measured stable pressures over the model predicted pressures, likely due to the venting effect. Despite being far from perfected, the prototype nevertheless showed much potential in becoming a useful device.

#### 3.3.1 Next Steps

One way that the battery design could be greatly improved is by having a seamless integration of the catalyst onto the piston, as shown in Fig. 3-16. This should be possible through a plating operation. If the piston o-ring was instead embedded in the body piston bore, when the battery's internal pressure increased, the change in pressure would physically begin to separate the catalyst from the reaction. The O-ring would essentially act as a squeegee, wiping solution off the piston catalyst as it exits the solution chamber.

This has a number of benefits. First, when the battery reaches its cut-off pressure, the catalyst will be completely removed from the reaction, ensuring that the observed venting effect does not occur, preventing significant pressure overshoot and immediately stopping the decomposition. The battery could be easily stored at zero gauge

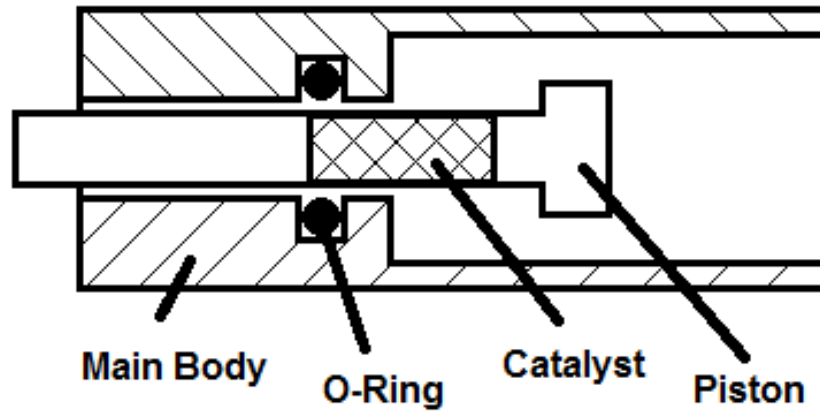


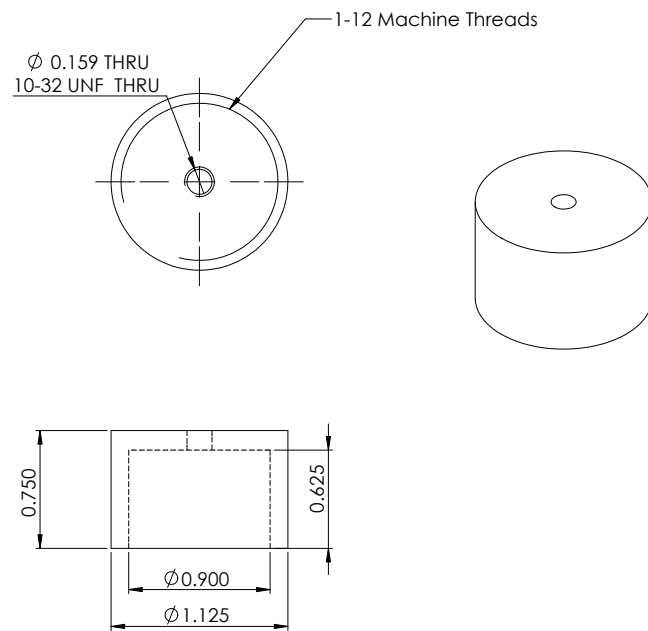
Figure 3-16: Sketch of an improved battery design.

pressure by orienting the piston such that the catalyst is completely out of contact with the solution. Additionally, because the surface area of exposed catalyst affects the rate of the decomposition, the decomposition rate can be compensated for despite having a decreasing concentration of potent solution. This could be especially useful if the outlet of the battery was constantly exposed to an external pressure, such as in a rocket. Any time the desired pressure would drop, the catalyst would become more exposed, increasing the rate of the decomposition and restoring the desired pressure. Last, because the catalyst diameter is the same as that of the piston, the ratio between the solution chamber diameter and the piston bore diameter can be much smaller, allowing the battery to become much more compact.

# Appendix A

## Prototype Part Drawings

Note: All drawings are in inches



SolidWorks Student License  
Academic Use Only

Figure A-1: Drawing of the cap.

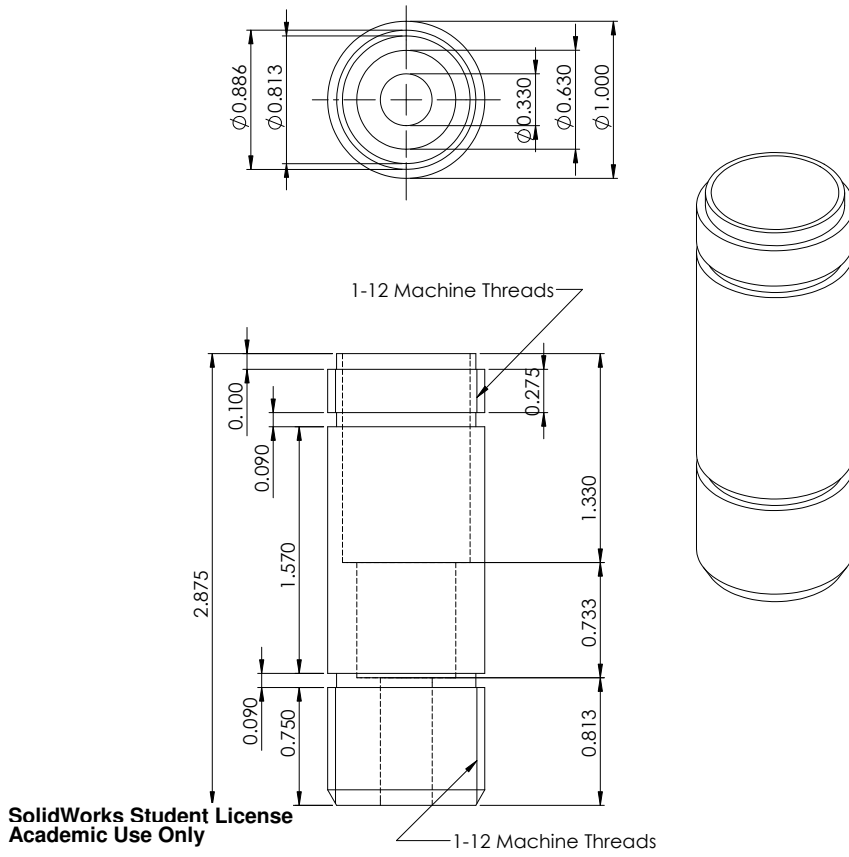
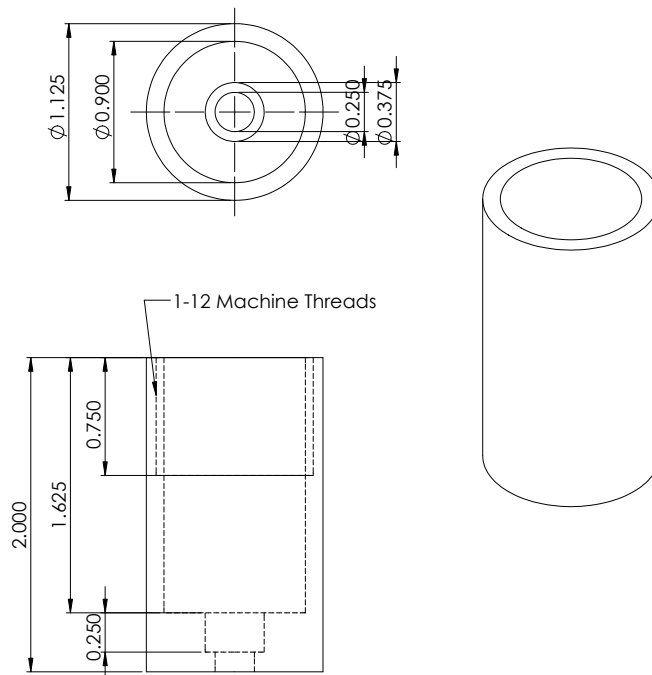
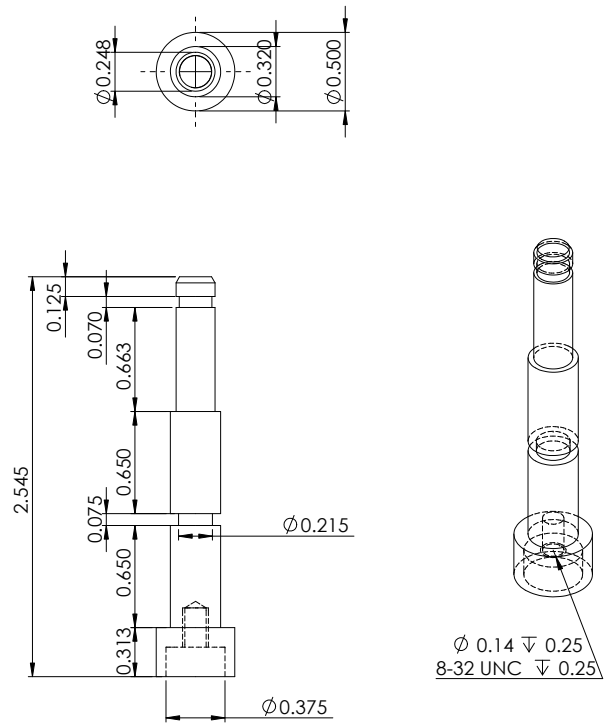


Figure A-2: Drawing of the main body.



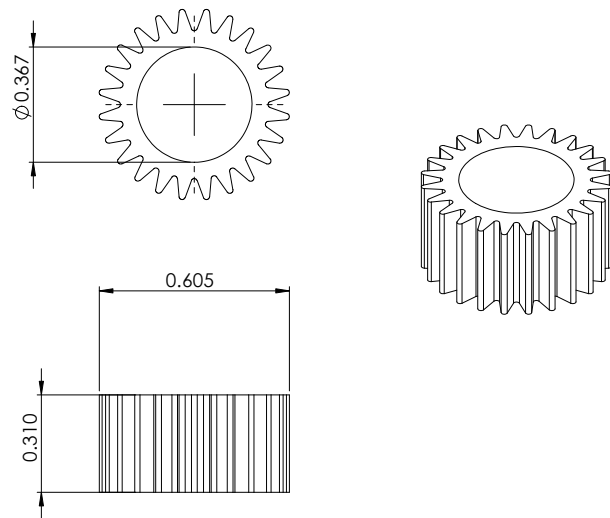
SolidWorks Student License  
Academic Use Only

Figure A-3: Drawing of the knob.



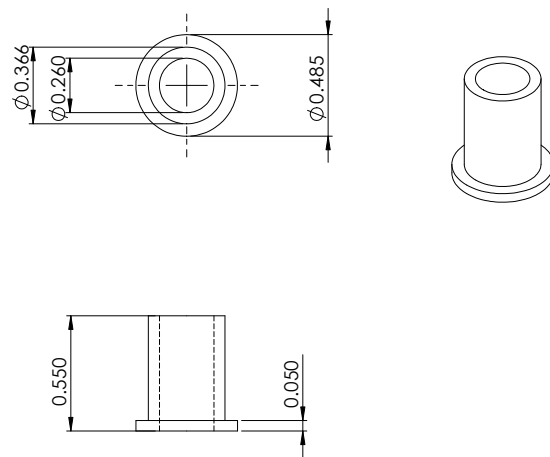
SolidWorks Student License  
Academic Use Only

Figure A-4: Drawing of the piston.



**SolidWorks Student License  
Academic Use Only**

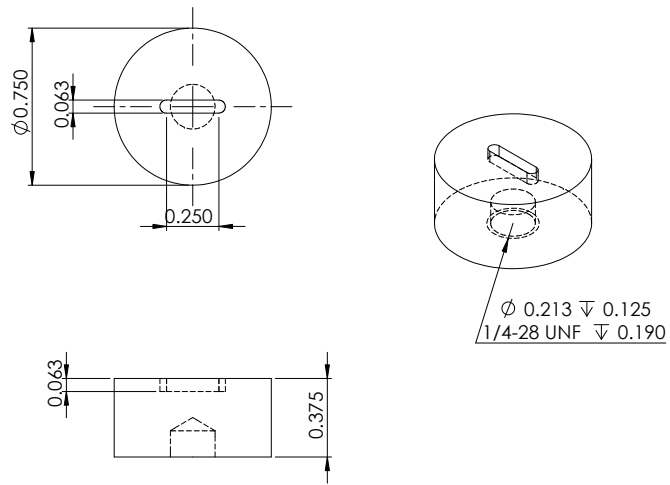
Figure A-5: Drawing of the Clear Care catalyst after turning.



SolidWorks Student License  
Academic Use Only

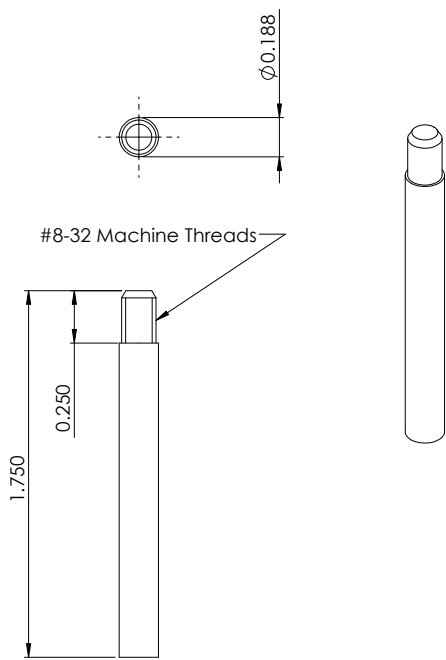
Figure A-6: Drawing of the catalyst mount.





SolidWorks Student License  
Academic Use Only

Figure A-7: Drawing of the catalyst cap.



SolidWorks Student License  
Academic Use Only

Figure A-8: Drawing of the pin.

# Bibliography

- [1] M. Goldfarb, E. J. Barth, M. A. Gogola, and J. A. Wehrmeyer. Design and energetic characterization of a liquid propellant powered actuator for self-powered robots. *IEEE/ASME Transactions of Mechatronics*, 8(2):264–262, Jun 2003.
- [2] H. Kazerooni. Design and analysis of pneumatic force generators for mobile robotic systems. *IEEE/ASME Transactions of Mechatronics*, 10(4):411–418, 2005.
- [3] C. D. Onal, X. Chen, G. M. Whitesides, and D. Rus. Soft mobile robots with on-board chemical pressure generation. In *International Symposium on Robotics Research (ISRR)*, 2011.
- [4] L. Qin, O. Vermesh, Q. Shi, and J. Heath. Self-powered microfluidic ships for multiplexed protein assays from whole blood. *Lab on a Chip*, 9(14):2016–2020, 2009.
- [5] I. A. Salem, M. El-Maazawi, and A. B. Zaki. Kinetics and mechanisms of decomposition reaction of hydrogen peroxide in presence of metal complexes. *International Journal of Chemical Kinetics*, 32(11):643–666.
- [6] F. Vitale. Low-temperature H<sub>2</sub>O<sub>2</sub>-powered actuators for biorobotics: Thermodynamic and kinetic analysis. In *Proceedings - IEEE International Conference on Robotics and Automation*, pages 2197–2202, 2010.
- [7] Y. Wang. Bipolar electrochemical mechanism for the propulsion of catalytic nanomotors in hydrogen peroxide solutions. *Langmuir*, 22(25):10451–10456, 2006.
- [8] J. C. Whitehead. Hydrogen peroxide propulsion for smaller satellites. In *AIAA/USU Conference on Small Satellite*, 1998.